Progress In Electromagnetics Research M, Vol. 3, 57–78, 2008

DESIGN OF A COMPACT PRINTED BAND-NOTCHED ANTENNA FOR ULTRAWIDEBAND COMMUNICATIONS

N. H. M. Sobli and H. E. Abd-El-Raouf

Department of Electrical and Computer Engineering
Faculty of Engineering
International Islamic University (IIUM)
53100 Kuala Lumpur, Malaysia

Abstract—A compact printed ultra-wideband (UWB) antenna with band-notched characteristic is presented. The antenna is designed to cover the Federal Communications Commission (FCC) bandwidth for UWB applications (3.1–10.6 GHz) with band-notched at frequency band (5.15–5.825 GHz). The proposed antenna is fed by microstrip line, and it consists of square radiating patch on the top layer with a slotted-parasitic patch on the bottom layer of the antenna. The slotted-parasitic patch acts as a notch filtering element to reject the frequency band (5.15–5.825 GHz) which is used by IEEE 802.11a and HIPERLAN/2. Moreover, the pulse distortions of different input pulses are investigated based on S_{21} parameters for two cases; face to face and side by side orientations. There is a small acceptable influence on the matching between the input and the output pulses and it is found that the pulse distortion is low. Therefore, the proposed antenna is a good candidate for UWB applications.

1. INTRODUCTION

In 2002, Federal Communication Commission (FCC) had released permission for commercial use of the frequency band from 3.1 to 10.6 GHz for radar, positioning, and data transmission [1]. Ultrawideband (UWB) radio is an emerging technology with attractive features useful for wireless communications, networking, radar processing, imaging and positioning [2]. Due to this extremely broad operating frequency range, antenna design for UWB communication applications is facing many challenges. One of them is to optimize the antenna to reduce the total size and weight of the communication

equipments with broad impedance bandwidth and high radiation efficiency [3]. Generally, UWB communication antennas require low voltage standing wave ratio (VSWR < 2), constant phase center, constant group delay, and constant gain over entire operating frequency band [3]. Printed monopole antennas can be considered as a good candidate for UWB applications due to their light weight, simple structure, and ease of mass production. In the design of a printed UWB antenna, the radiator and the ground plane shapes as well as the feeding structure can be optimized to achieve a good broad impedance bandwidth [4–12]. In addition, time domain analysis of UWB antenna plays an important role to determine pulse distortion of the received signal [13–16].

However, existing Wireless Local Area Network (WLAN), IEEE 802.11a systems operating in the frequency band (5.15–5.825 GHz) can cause interference with UWB systems. Therefore, a band stop filter that rejects this limited bandwidth would be required in UWB RF front-ends to reduce the inference between the UWB system and these systems. To avoid adding new circuits to the communication system, band-notching technique can be applied directly to various UWB antennas [17]. Therefore, many antennas with band rejection characteristic have been researched with the utilization of advantages of composing more simply RF front-ends. Different configurations for band notching are introduced such as U-shape, V-shape and I-shape [18–23].

In this paper, a new compact UWB patch antenna with a band-notching is presented. The band-notching is obtained by introducing slotted-parasitic patch on the bottom layer of the antenna. This slotted-parasitic patch will act as a band stop filter to eliminate WLAN frequency band. In the present design, three steps are used, W-shaped slot on the patch, and a slit is introduced on the partial ground plane to increase the operating bandwidth. Then a slotted-parasitic patch is added on the bottom layer of the antenna to introduce the band-notching effect. Section 2 presents the details of the antenna structure. Full wave analysis of the proposed antennas in frequency domain is obtained by using CST Microwave Studio and Ansoft HFSS which are based on Finite Integration Method and Finite Element Method respectively. The return loss and far-field results obtained are presented in Section 3 and Section 4 presents the time domain response of the proposed antennas. Finally, Section 5 presents the correlation between the transmitting and the receiving antennas.

2. ANTENNA DESIGN

Figure 1 shows the geometry of the proposed antenna, with a W-shaped slot on the radiating patch. The patch has the form of a rectangle with a three steps at its lower end to improve the matching of the antenna over the operating bandwidth. A partial ground plane with a slit is used on the other side of the substrate. The total size of the antenna is 30 mm × 35 mm with metal thickness of 0.07 mm. The used substrate is FR4 which has dielectric constant, $\varepsilon_r = 4.4$ and its thickness, $h = 1.57$ mm.

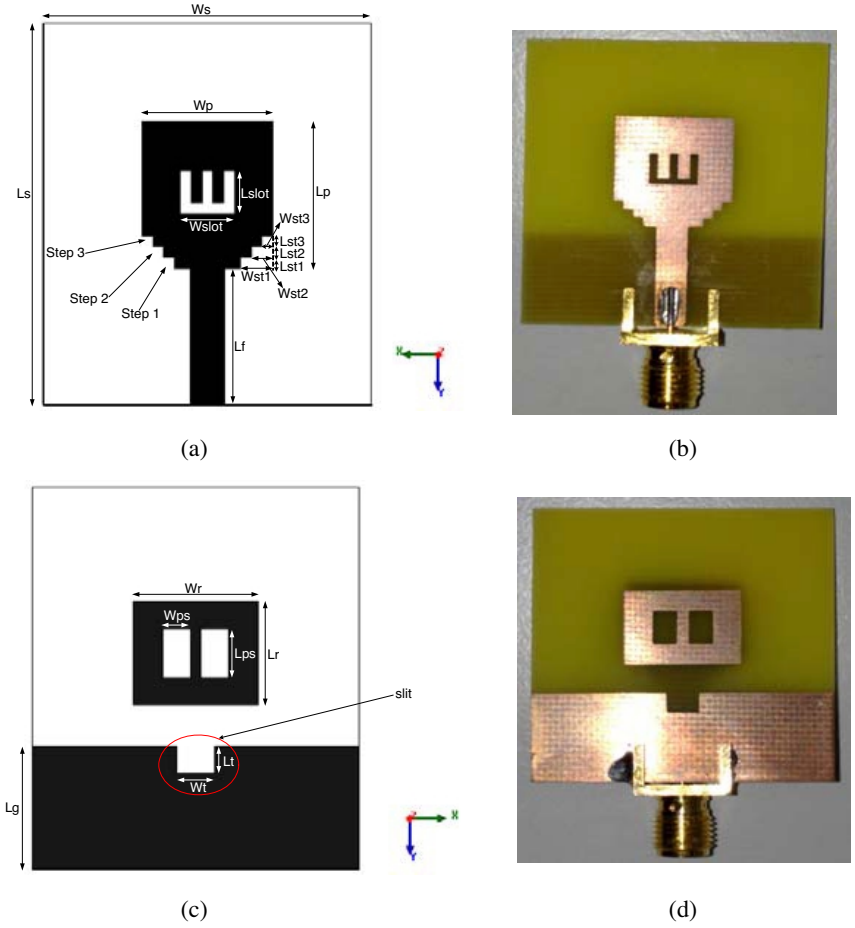

Figure 1. Geometry and configuration of the proposed antenna: (a) top layer view, (b) fabricated antenna top layer view, (c) bottom layer view, (d) fabricated antenna bottom layer view.

The dimensions of the rectangular patch are 12 mm×13.5 mm with slot's dimension of $W_{slot} = 5$ mm and $L_{slot} = 3$ mm. The dimensions of the partial ground plane are chosen to be 30 mm × 11.2 mm with slit's dimensions of 3.5 mm × 2.5 mm. The dimensions of the parasitic rectangular patch are 11.5 mm×9.5 mm which is printed on the bottom layer of the antenna. The slots on the parasitic patch have dimension of 2.5 mm × 4.5 mm each. The length of the microstrip line is 12.5 mm. The antenna has the following parameters: $L_s = 35$ mm, $W_s = 30$ mm, $L_p = 13.5$ mm, $W_p = 12$ mm, $L_{slot} = 3$ mm, $W_{slot} = 5$ mm, $L_r = 9.5$ mm, $W_r = 11.5$ mm, $W_{ps} = 2.5$ mm, $L_{ps} = 4.5$ mm, $W_t = 3.5$ mm, $L_t = 2.5$ mm, $L_f = 12.5$ mm, and $L_g = 11.2$ mm. The dimensions of the three steps are as follows: Step 1 ($W_{st1} = 3$ mm, $L_{st1} = 1$ mm), Step 2 ($W_{st2} = 2$ mm, $L_{st2} = 1$ mm), and Step 3 ($W_{st3} = 1$ mm, $L_{st3} = 1$ mm). We have obtained these dimensions after a parametric study using CST Microwave Studio and Ansoft HFSS. The antenna is fabricated and the return loss of the antenna is measured by using Agilent E8364B PNA Network Analyzer. To design the band-notched UWB antenna, four techniques had been applied to the proposed antenna: the use of (i) three steps (ii) partial ground plane with slit, (iii) slotted-parasitic patch on the bottom layer of the antenna, and (iv) W-shaped slots on the radiating patch which can lead to a good impedance matching as well as band notching at 5.15–5.825 GHz. By selecting these parameters, the proposed antenna can be tuned to operate in the 3.1–10.6 GHz frequency range with band rejection (5.15–5.825 GHz).

3. RETURN LOSS AND FAR-FIELD RESULTS

Figure 2 to Figure 9 show the parametric study on the return loss of the proposed antenna. Figure 2 shows the effect of step widths, W_{st1}, W_{st2}, and W_{st3} on the return loss of the proposed antenna without slotted-parasitic patch. The figure shows that by increasing the step widths of the proposed antenna, the return loss will also increase above than −10 dB. The optimum dimensions for step widths are $W_{st1} = 3$ mm, $W_{st2} = 2$ mm, and $W_{st3} = 1$ mm. Figure 3 shows the effect of the ground plane length, L_g on the return loss of the proposed antenna without slotted-parasitic patch. The figure shows that the ground plane length sensitive to the input impedance over the entire UWB band. The optimum ground plane length is $L_g = 11.2$ mm. To further reduce the return loss to be below than −10 dB and increase the bandwidth of the proposed antenna, a slit is introduced on the ground plane. Figure 4 shows that slit length L_t, influences the input impedance at frequency 9 GHz and above

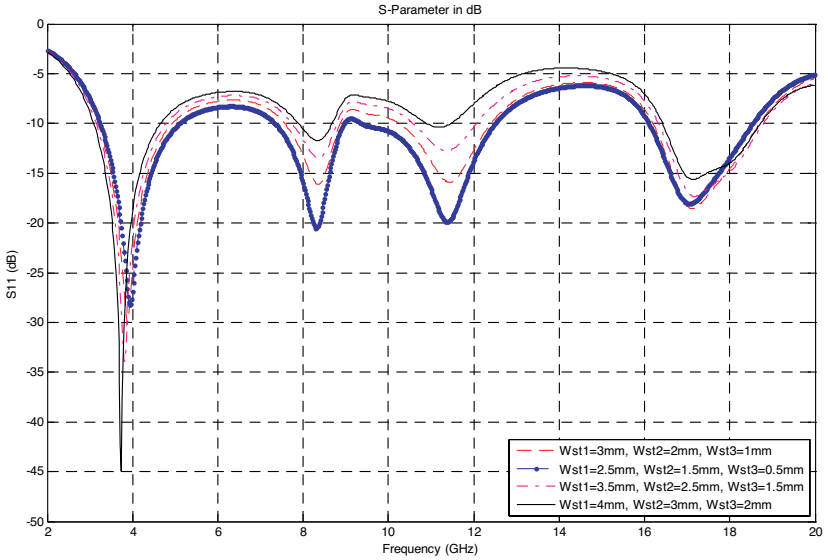

Figure 2. Effect of step widths, W_{st1}, W_{st2}, and W_{st3} on the return loss of the proposed antenna.

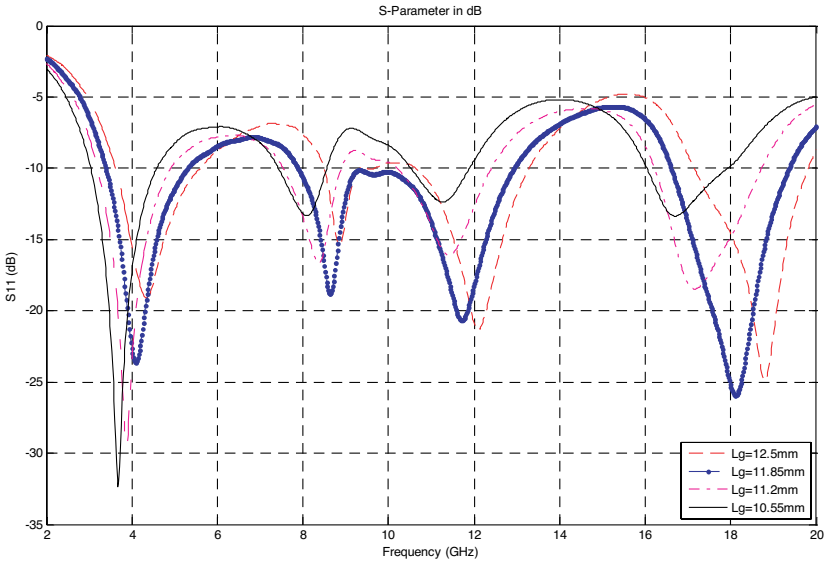

Figure 3. Effect of ground plane length, L_g on the return loss of the proposed antenna.

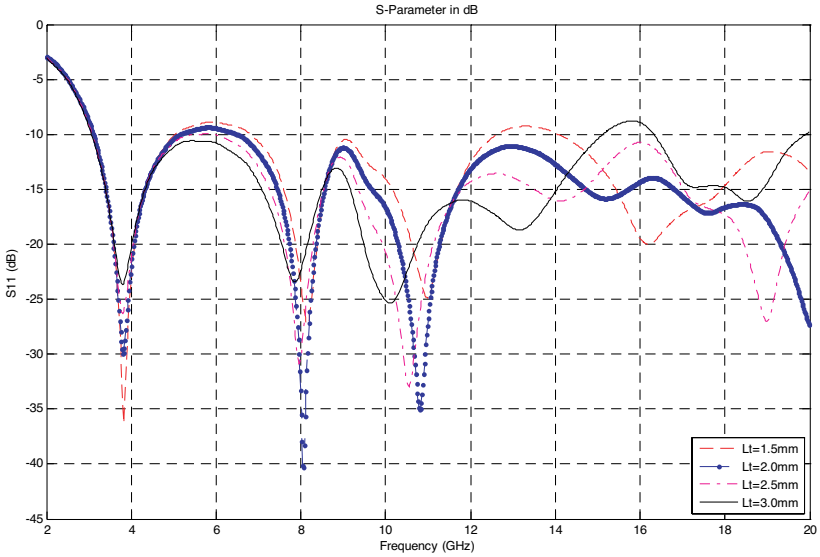

Figure 4. Effect of ground slit length, L_t on the return loss of the proposed antenna.

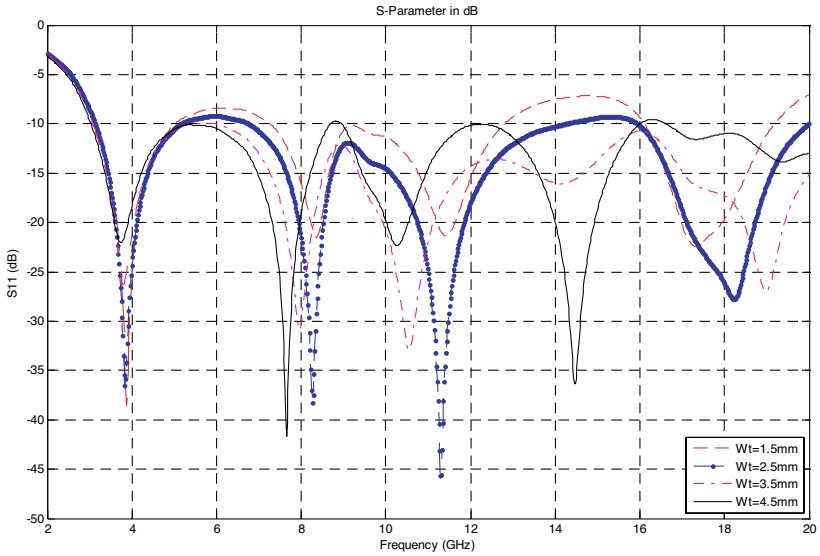

Figure 5. Effect of ground slit width, W_t on the return loss of the proposed antenna.

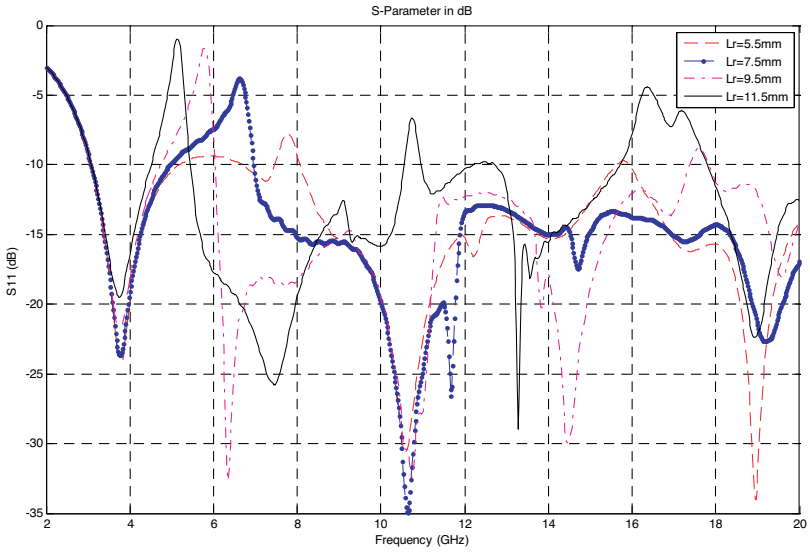

Figure 6. Effect of parasitic element length, L_r on the return loss of the proposed antenna.

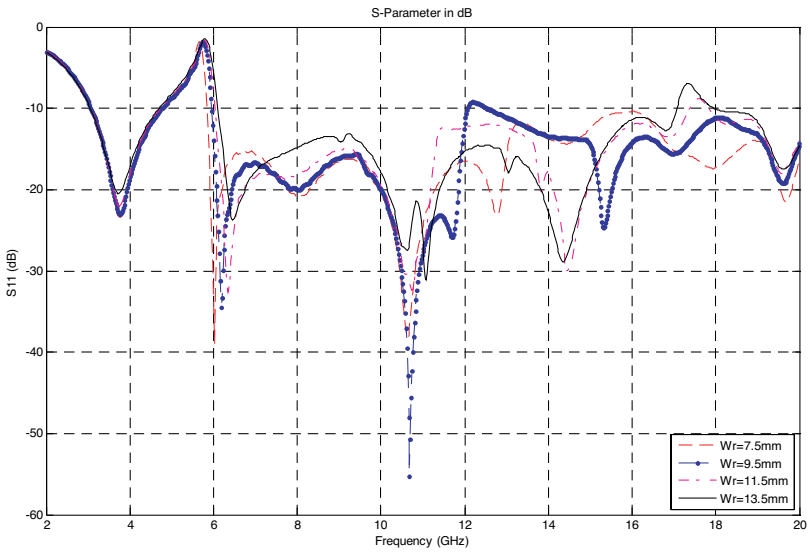

Figure 7. Effect of parasitic element width, W_r on the return loss of the proposed antenna.

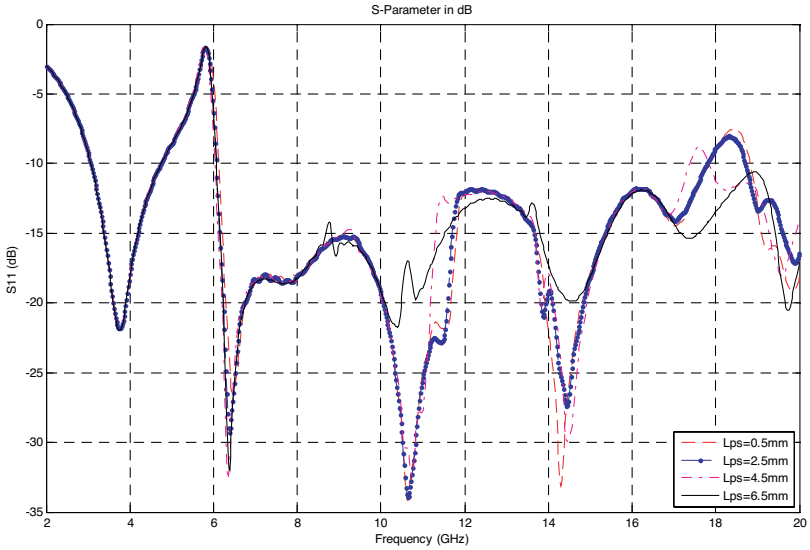

Figure 8. Effect of parasitic element slot length, L_{ps} on the return loss of the proposed antenna.

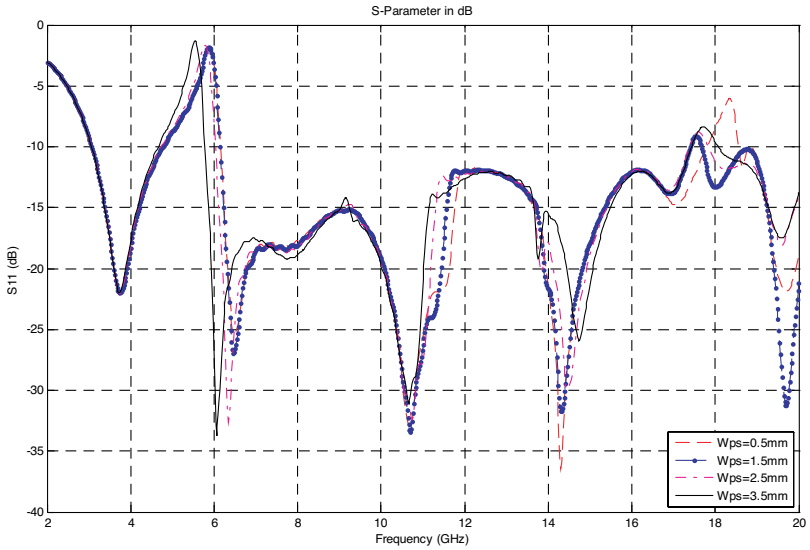

Figure 9. Effect of parasitic element slot width, W_{ps} on the return loss of the proposed antenna.

while slit width W_t influences the input impedance from 6 GHz and above as shown in Figure 5. The optimum dimensions for the slit are $L_t = 2.5$ mm and $W_t = 3.5$ mm. In order to reject frequency band (5.15–5.825 GHz) for WLAN applications, a slotted-parasitic patch is introduced at the bottom layer of the proposed antenna. Figure 6 shows the effect of parasitic patch length on the return loss of the proposed antenna. The figure shows that the parasitic patch length, L_r influences the input impedance at the notched frequency band as well as the input impedance over the entire UWB band. Figure 7 shows the effect of parasitic patch width, W_r on the return loss of the proposed antenna. From those figures, the optimum dimensions for the parasitic patch are $L_r = 9.5$ mm and $W_r = 11.5$ mm. Figure 8 shows that the parasitic slot length L_{ps} can control the input impedance at notched frequency around 6 GHz while the parasitic slot width W_{ps} in Figure 9 influences the bandwidth of the notched frequency. From those figures, the optimum dimension for the slot on the parasitic patch are $L_{ps} = 4.5$ mm and $W_{ps} = 2.5$ mm. Therefore, from the parametric study, it is shown that the input impedance bandwidth and notched frequency of the proposed antenna can be controlled by properly choose its parameters values.

Figure 10 shows the simulated return loss from CST and HFSS

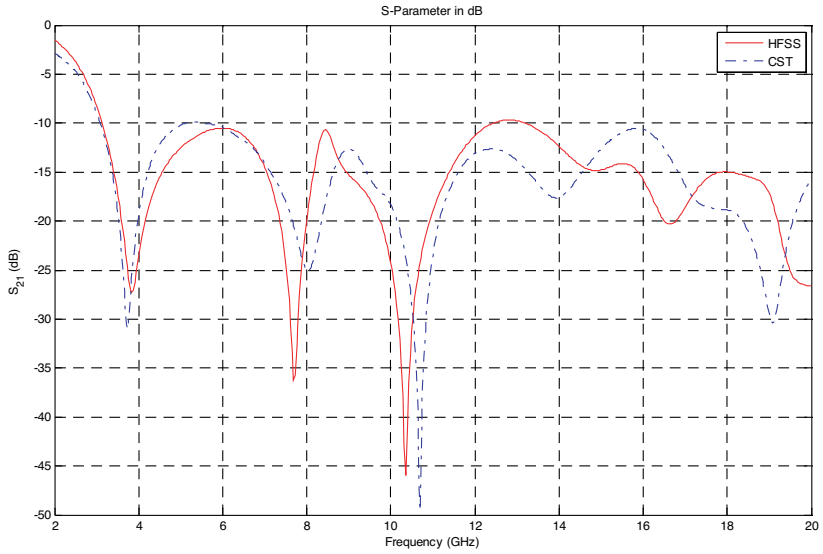

Figure 10. Simulated return loss of the proposed antenna without slotted parasitic element.

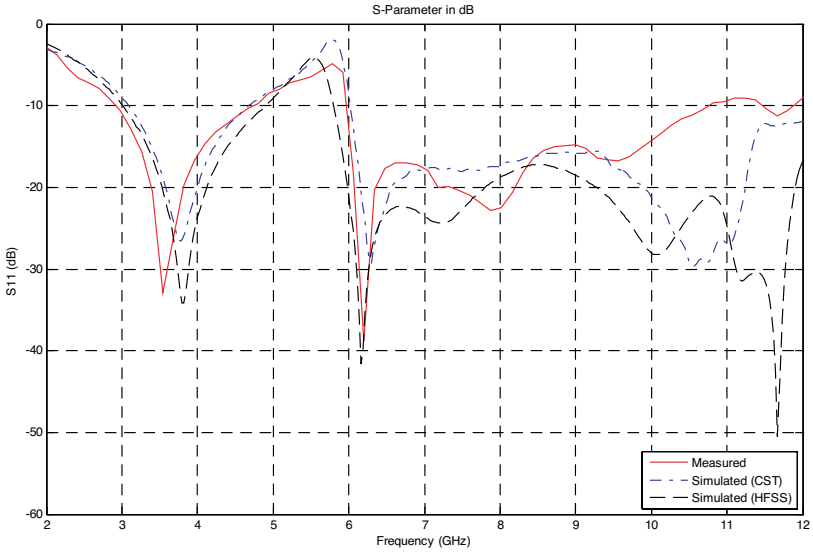

(a)

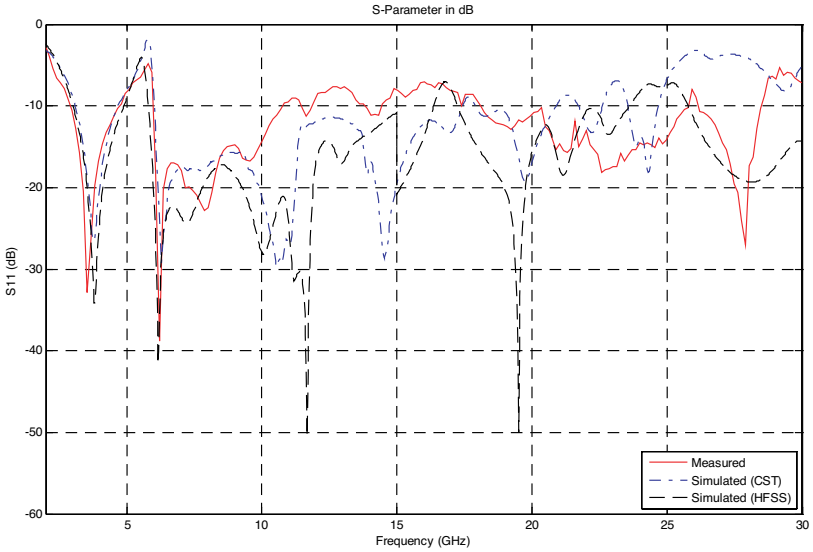

(b)

Figure 11. Simulated and measured return loss (a) from 2–12 GHz (b) from 2–30 GHz.

of the proposed antenna without slotted-parasitic patch. The figure shows that the proposed antenna satisfies the UWB frequency band for return loss below −10 dB. Figure 11 shows the simulated and measured return loss of the proposed antenna with slotted-parasitic patch for the frequency bands (a) 2 GHz–12 GHz and (b) 2 GHz–30 GHz. The simulation is done by using CST Microwave Studio and Ansoft HFSS. The fabricated antenna is measured by using Agilent E8364B PNA Network Analyzer. It is shown from the figure that the proposed antenna can satisfy return loss below −10 dB for the UWB band according to CST (3.09–17.43 GHz), HFSS (3.01–16.36 GHz) and the measured is (2.92–10.75 GHz) with band rejection CST (5.15–5.99 GHz), HFSS (5.16–5.75 GHz) and the measured is (5.16 to 5.95 GHz). Therefore the slotted-parasitic patch introduces high return loss within the required rejection band.

Figure 12(a) shows the total gain of the proposed antenna versus the frequency. The figure shows that the proposed antenna's gain variates between 0.5 dB and 6.174 dB within the operating frequency band of the antenna. Figure 12(b) shows the radiation efficiency of the proposed antenna versus the frequency. The efficiency variates between 74.49% and 95.03% within the operating frequency band except for the band notched in which the efficiency is 32.31%. Figure 12(c) shows the directivity of the proposed antenna versus the frequency. It shows that the antenna's directivity variates between 1 dBi to 6.5 dBi within the operating frequency band of the antenna.

Figure 13 shows the radiation pattern of the proposed antenna in the YZ-plane and in the XZ-plane at the frequencies 3.1 GHz, 6.5 GHz, and 10 GHz. The antenna is located in the YZ-plane with maximum radiation on X-axis. The figure shows that the radiation pattern of the proposed antenna at lower frequency (i.e., 3.1 GHz and 6.5 GHz) is omni-directional in the XZ-plane and quasi omni-directional in the YZ-plane. Meanwhile, at higher frequency (i.e., 10 GHz), the radiation pattern is quite distorted in both planes. The figure also shows that the cross-polarization effect on the radiation pattern is acceptable at lower frequency but it is getting bigger at higher frequency in both planes.

4. TIME DOMAIN RESPONSE

In this section, we consider the communication between two of the designed band-notched UWB antennas. The distance between the transmitting and the receiving antennas is 60 cm, which is approximately 6 wavelengths at the lowest frequency of the considered band of operation. Therefore, we assume that the antennas are in the

far field of each other.

The transmitting antenna is excited with different input pulses which are first order Rayleigh pulse, fourth order Rayleigh pulse, modulated Gaussian pulse and fifth derivative of Gaussian pulse. Those source pulses are selected with different values of pulse characteristic time, a in order to ensure that the shape of the spectrum complies with FCC spectral mask. We assume that the antennas operate in two orientations: (a) face to face and (b) side by side as shown in Figure 14.

Figure 15 shows the transfer function, S_{21} versus the frequency in two different orientations. From the figure it shows that the transfer function of face to face orientations is better than that of side by side either with parasitic patch or without parasitic patch. Figure 16 shows the comparison of the received and the input pulses for different source signals for two different orientations of the proposed antenna. The received pulse is obtained by convoluting the system impulse response with the input pulse and then each of the input pulse and the output pulse is normalized to its peak value. From the Figure 16 it shows that the input pulses main beam are not distorted but ripples appear, lengthening the received pulse.

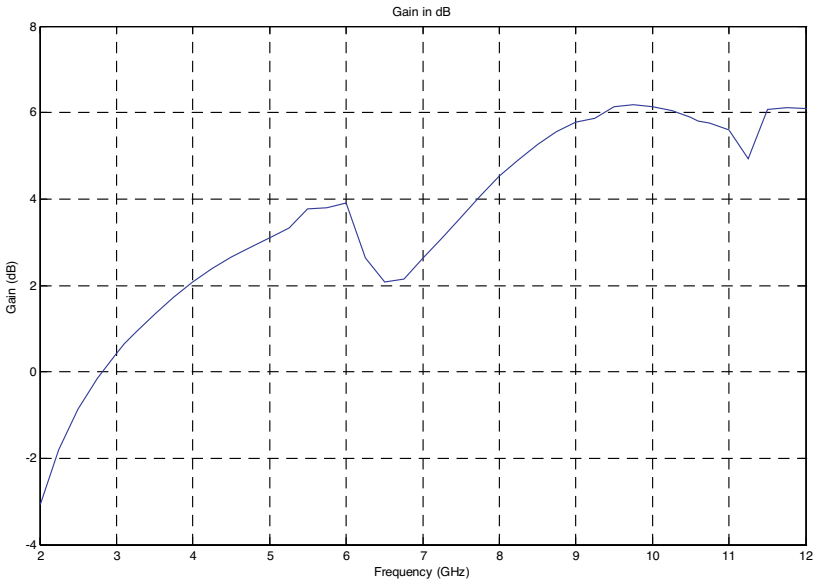

(a)

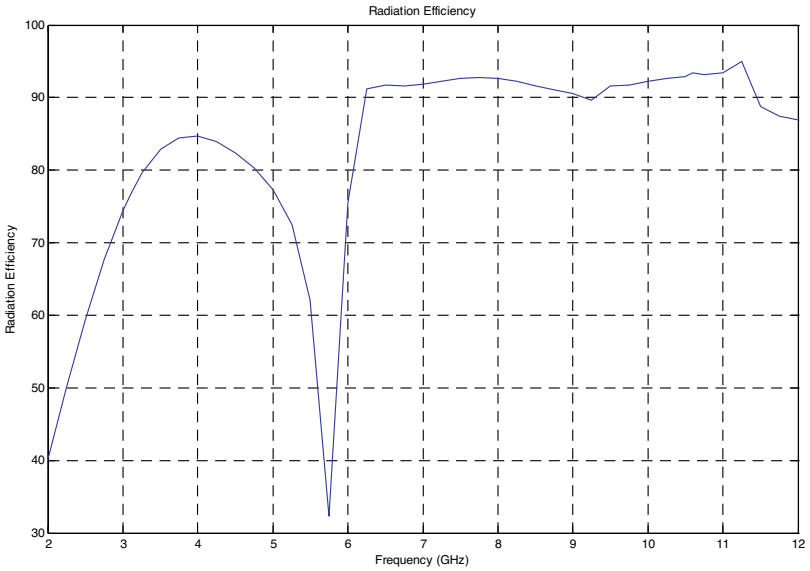

(b)

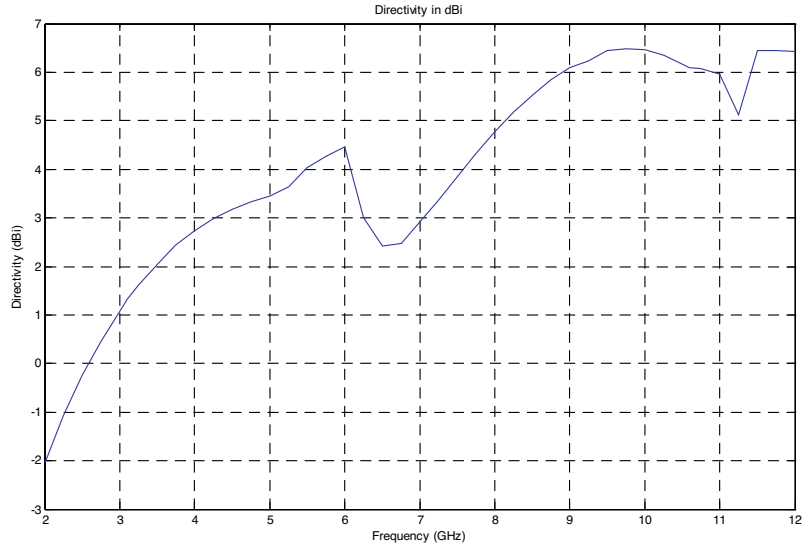

(c)

Figure 12. (a) Gain, (b) radiation efficiency, (c) directivity of the proposed antenna.

5. THE CORRELATION BETWEEN THE TRANSMITTING AND THE RECEIVING ANTENNAS

The fidelity as given in the Equation (1) of the various source pulses are calculated for different antenna orientations and are tabulated in Table 1 (without slotted-parasitic patch) and Table 2 (with slotted-parasitic patch). According to the table, fidelity greater than 0.9 is

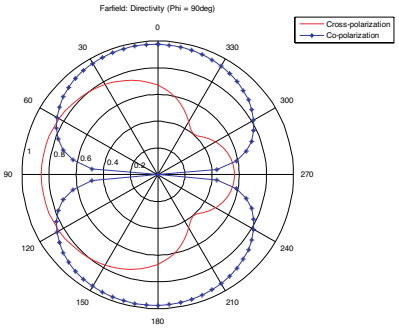

(a) YZ-plane at 3.1GHz

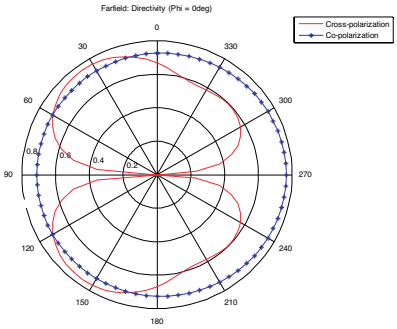

(b) XZ-plane at 3.1GHz

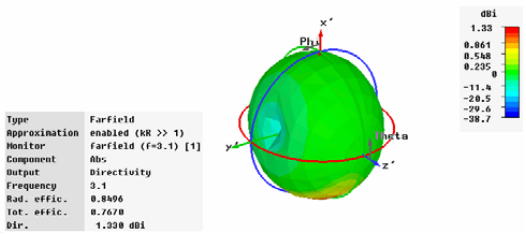

(c) Directivity at 3.1GHz

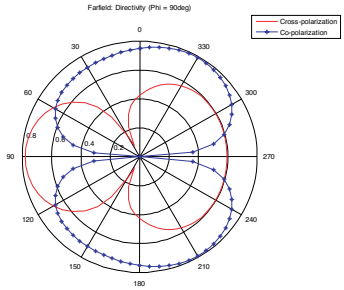

(d) YZ-plane at 6.5GHz

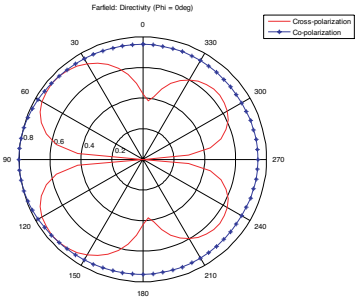

(e) XZ-plane at 6.5GHz

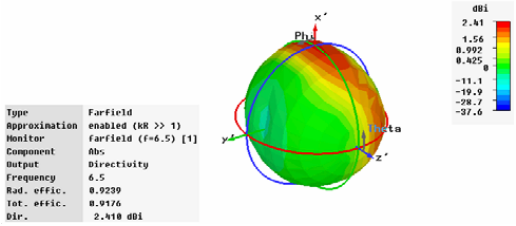

(f) Directivity at 6.5GHz

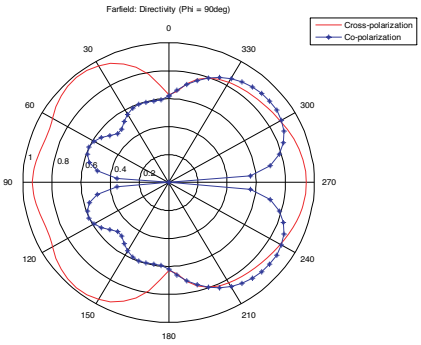

(g) YZ-plane at 10GHz

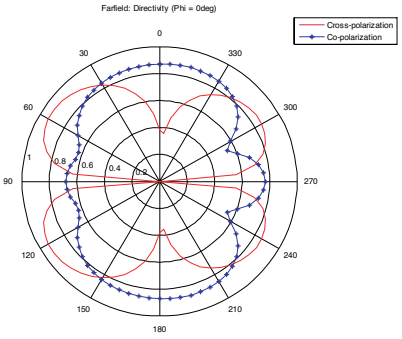

(h) XZ-plane at 10GHz

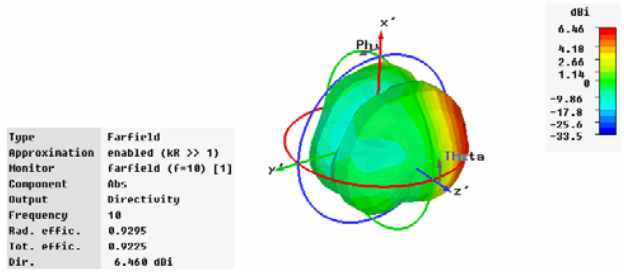

(i) Directivity at 10GHz

Figure 13. Radiation pattern of the proposed antenna in the YZ-plane ($\phi = 90°$) and the XZ-plane ($\phi = 0°$) at 3.1 GHz, 6.5 GHz and 10 GHz.

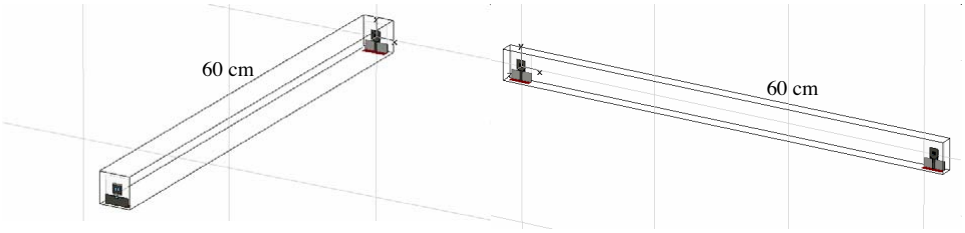

(a) Face to face (b) Side by side

Figure 14. Transmitting and Receiving antennas in two different orientations.

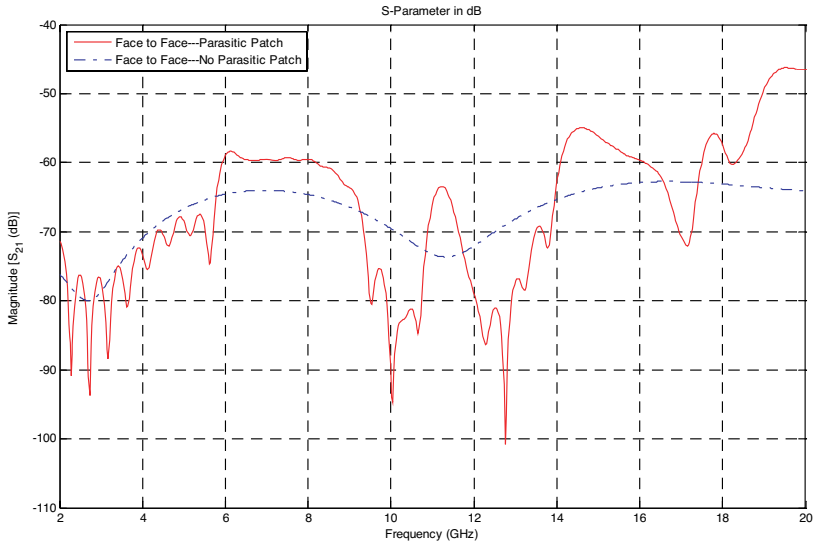

(a) Face to face

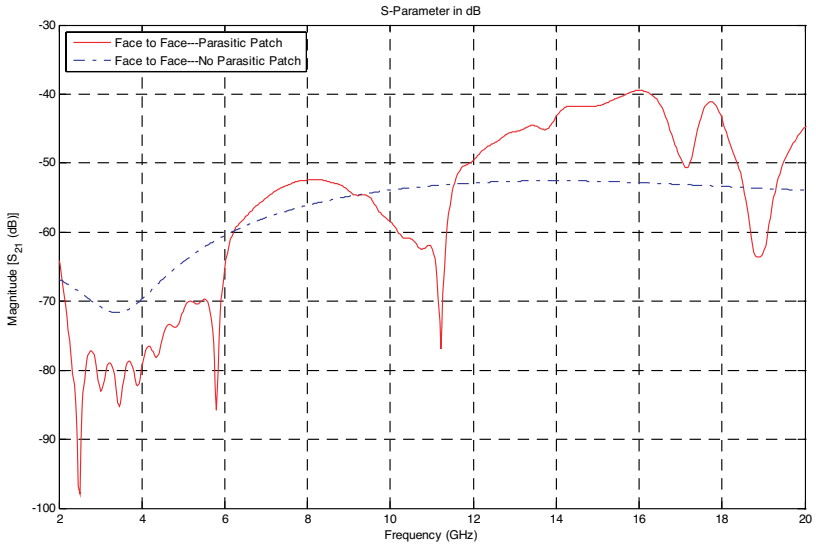

(b) Side by side

Figure 15. The transfer function, S_{21} (f) in two different orientations.

always achieved for all input signals. It is even better than 0.97 for fifth derivative Gaussian signal in both of two orientations.

$$F = \max_{\tau} \left[\frac{\int_{-\infty}^{+\infty} f(t) s_R(t+\tau) dt}{\sqrt{\int_{-\infty}^{+\infty} f^2(t) dt \int_{-\infty}^{+\infty} s_R^2(t) dt}} \right] \tag{1}$$

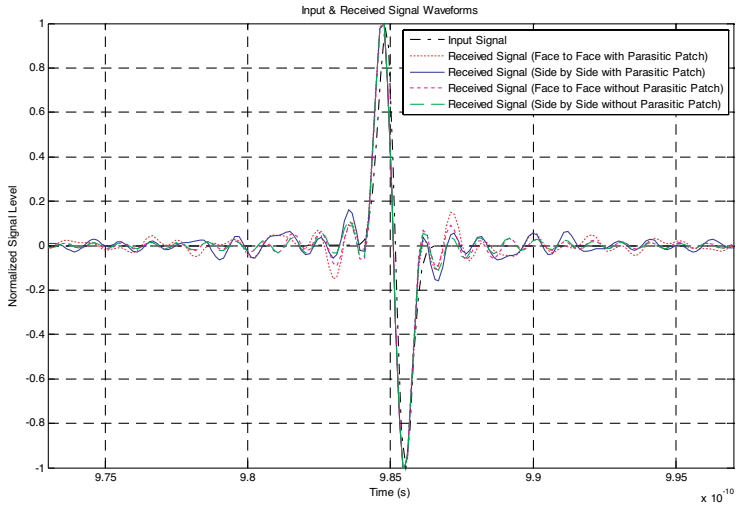

(a)

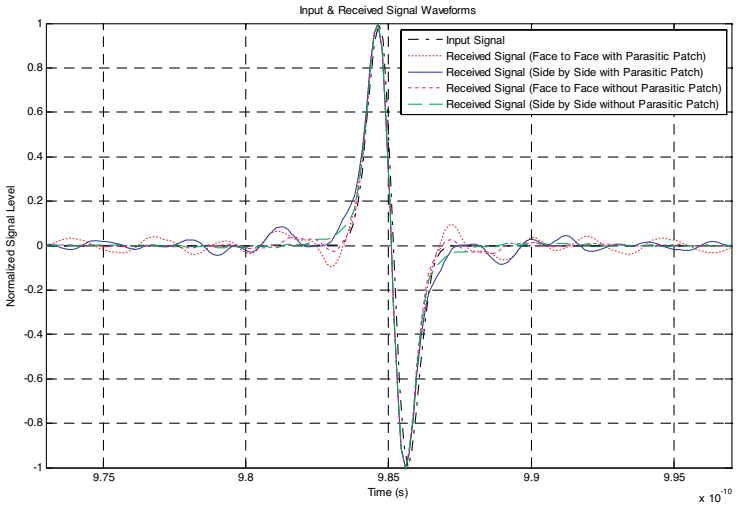

(b)

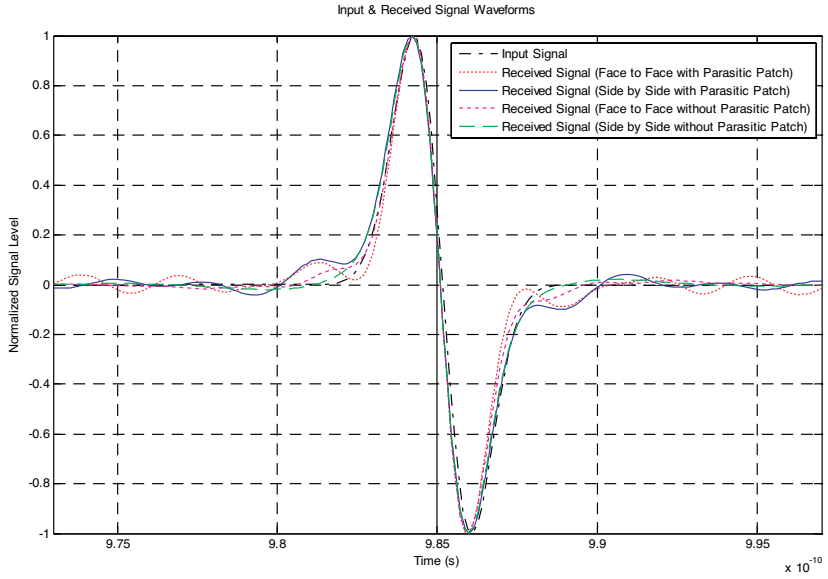
Input & Received Signal Waveforms
Input Signal
Received Signal (Face to Face with Parasitic Patch)
Received Signal (Side by Side with Parasitic Patch)
Received Signal (Face to Face without Parasitic Patch)
Received Signal (Side by Side without Parasitic Patch)
Normalized Signal Level
Time (s)
x 10^-10

(c)

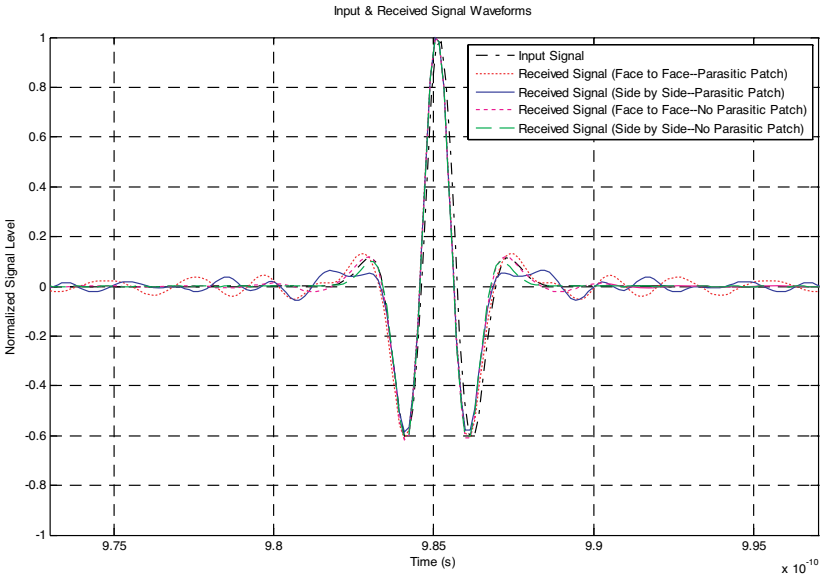
Input & Received Signal Waveforms
Input Signal
Received Signal (Face to Face--Parasitic Patch)
Received Signal (Side by Side--Parasitic Patch)
Received Signal (Face to Face--No Parasitic Patch)
Received Signal (Side by Side--No Parasitic Patch)
Normalized Signal Level
Time (s)
x 10^-10

(d)

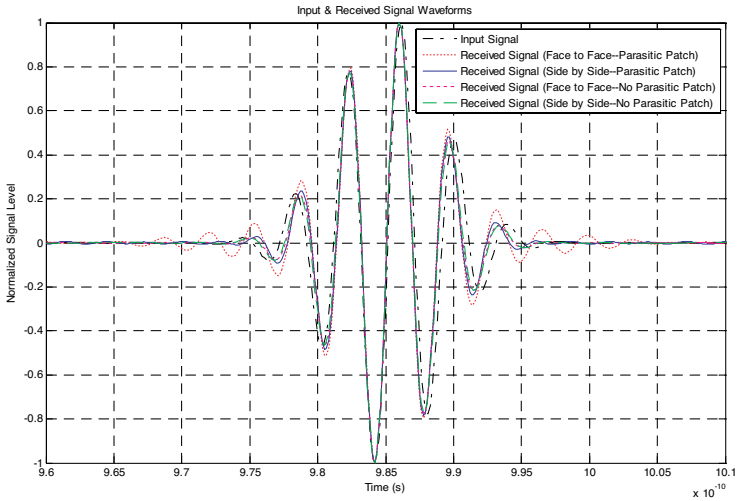

(e)

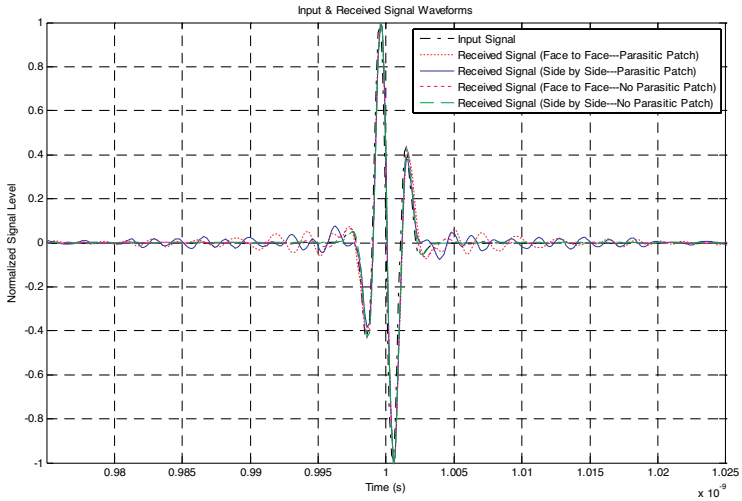

(f)

Figure 16. Comparison of the normalized received and input pulses for the different sources: (a) 1st Order Rayleigh Pulse when $a = 30\,\text{ps}$, (b) 1st Order Rayleigh Pulse when $a = 45\,\text{ps}$, (c) 1st Order Rayleigh Pulse when $a = 80\,\text{ps}$, (d) 4th Order Rayleigh Pulse when $a = 67\,\text{ps}$, (e) Modulated Gaussian Pulse when $a = 350\,\text{ps}$, (f) 5th Derivative Gaussian Pulse when $a = 51\,\text{ps}$ for two different orientations of the proposed antenna.

Table 1. Fidelity for proposed band-notched UWB antenna pair without slotted-parasitic patch.

	1st Order Rayleigh a = 30ps	1st Order Rayleigh a = 45ps	1st Order Rayleigh a = 80ps	4th Order Rayleigh a = 67ps	Modulate Gaussian a = 350ps	5th Derivative Gaussian a = 51ps
Face to Face	0.9559	0.9599	0.9690	0.9789	0.9875	0.9895
Side by Side	0.9533	0.9567	0.9631	0.9697	0.9780	0.9785

Table 2. Fidelity for proposed band-notched UWB antenna pair.

	1st Order Rayleigh a = 30ps	1st Order Rayleigh a = 45ps	1st Order Rayleigh a = 80ps	4th Order Rayleigh a = 67ps	Modulate Gaussian a = 350ps	5th Derivative Gaussian a = 51ps
Face to Face	0.9547	0.9589	0.9679	0.9777	0.9854	0.9887
Side by Side	0.9511	0.9557	0.9599	0.9684	0.9763	0.9779

6. CONCLUSION

A compact printed UWB antenna has been presented. A rectangular slotted parasitic patch has been used to obtain the band rejected characteristics. The proposed antenna exhibits a broad bandwidth with small size of $30\,\text{mm} \times 35\,\text{mm} \times 1.27\,\text{mm}$. The gain and the return loss of the antenna are satisfactory within the desired frequency band. The comparison of the results of CST, HFSS, and the measurements frequency band ($S_{11} < -10\,\text{dB}$) is from 3.09 to 10.75 GHz. The pulse distortion of the proposed antenna with various input signals was also studied and compared for two different orientations (face to face and side by side). The proposed band-notched antenna gives good results and it is well suited for UWB communications.

REFERENCES

1. New Public Safety Applications and Broadband Internet Access among Uses Envisioned by FCC Authorization of Ultra-Wideband Technology — FCC News Release 2002.

2. Yang, L. and G. B. Giannakis, "Ultra-wideband communications: An idea whose time has come," *IEEE Signal Processing Magazine*, Vol. 21, No. 6, 26–54, 2004.
3. Chen, Z. N., X. H. Wu, H. F. Li, N. Yang, and M. Y. W. Chia, "Consideration for source pulses antennas in UWB radio systems," *IEEE Transactions on Antennas and Propagation*, Vol. 52, No. 7, 1739–1748, 2004.
4. Wu, X. H., Z. N. Chen, and M. Y. W. Chia, "Note on antenna design in UWB wireless communication systems," *IEEE Conference on Ultra Wideband Systems and Technologies*, 503–507, 2003.
5. Suh, S.-Y., W. L. Stutzman, and W. A. Davis, "A new ultrawideband printed monopole antenna: The planar inverted cone antenna (PICA)," *IEEE Transactions on Antennas and Propagation*, Vol. 52, No. 5, 1361–1364, 2004.
6. Chen, Z. N., T. S. P. See, and X. Qing, "Small printed ultrawideband antenna with reduced ground plane effect," *IEEE Transactions on Antennas and Propagation*, Vol. 55, No. 2, 383–388, 2007.
7. Chair, R., A. A. Kishk, K.-F. Lee, C. E. Smith, and D. Kajfez, "Microstrip line and CPW FED ultra wideband slot antennas with U-shaped tuning stub and reflector," *Progress In Electromagnetics Research*, PIER 56, 163–182, 2006.
8. Eldek, A. A., A. Z. Elsherbeni, and C. E. Smith, "Rectangular slot antenna with patch stub for ultra wideband applications and phased array systems," *Progress In Electromagnetics Research*, PIER 53, 227–237, 2005.
9. Klemm, M. and G. Troester, "EM energy absorption in the human body tissues due to UWB antennas," *Progress In Electromagnetics Research*, PIER 62, 261–280, 2006.
10. Zaker, R., C. Ghobadi, and J. Nourinia, "A modified microstrip-FED two-step tapered monopole antenna for UWB and WLAN applications," *Progress In Electromagnetics Research*, PIER 77, 137–148, 2007.
11. Sadat, S., M. Houshmand, and M. Roshandel, "Design of a microstrip square-ring slot antenna filled by an H-shape slot for UWB applications," *Progress In Electromagnetics Research*, PIER 70, 191–198, 2007.
12. Sadat, S., M. Fardis, F. G. Kharakhili, and G. Dadashzadeh, "A compact microstrip square-ring slot antenna for UWB applications," *Progress In Electromagnetics Research*, PIER 67, 173–179, 2007.

13. Marrocco, G., M. Migliorelli, and M. Ciattaglia, "Simultaneous time-frequency modeling of ultra-wideband antennas by two-dimensional hermite processing," *Progress In Electromagnetics Research*, PIER 68, 317–337, 2007.
14. Mehdipour, A., K. Mohammadpour-Aghdam, and R. Faraji-Dana, "Complete dispersion analysis of vivaldi antenna for ultra wideband applications," *Progress In Electromagnetics Research*, PIER 77, 85–96, 2007.
15. Eldek, A. A., "Numerical analysis of a small ultra wideband microstrip-FED tap monopole antenna," *Progress In Electromagnetics Research*, PIER 65, 59–69, 2006.
16. Akhoondzadeh-Asl, L., M. Fardis, A. Abolghasemi, and G. Dadashzadeh, "Frequency and time domain characteristic of a novel notch frequency UWB antenna," *Progress In Electromagnetics Research*, PIER 80, 337–348, 2008.
17. Zhang, G.-M., J.-S. Hong, and B.-Z. Wang, "Two novel band-notched UWB slot antennas FED by microstrip line," *Progress In Electromagnetics Research*, PIER 78, 209–218, 2008.
18. Peyrot-Solis, M. A., J. A. Tirado-Mendez, and H. Jardon-Aguilar, "Design of multiband UWB planarized monopole using DMS technique," *Antennas and Wireless Propagation Letters*, Vol. 6, 77–79, 2007.
19. Su, S. W., K. L. Wong, and F. S. Chang, "Compact printed band-notched ultrawideband slot antenna," *IEEE Antennas and Propagation Society International Symposium*, Vol. 2B, 572–575, 2005.
20. Kim, Y. and D. H. Kwon, "CPW-fed planar ultra wideband antenna having a frequency band notch function," *Electronics Letters*, Vol. 40, No. 7, 403–405, 2004.
21. Yoon, H., H. Kim, K. Chang, Y. J. Yoon, and Y. H. Kim, "A study on the UWB antenna with band-rejection characteristic," *IEEE Antennas Propagation Society International Symposium*, Vol. 2, 1784–1787, Monterey, CA, 2004.
22. Yoon, I. J., H. Kim, H. K. Yoon, Y. J. Yoon, and Y. H. Kim, "Ultra-wideband tapered slot antenna with band cutoff characteristic," *Electronics Letters*, Vol. 41, No. 11, 629–630, 2005.
23. Kim, Y. and D. H. Kwon, "Planar ultra wide band slot antenna with frequency band notch function," *IEEE Antennas Propagation Society International Symposium*, 1788–1791, Monterey, CA, 2004.